A Simple Approach to Near-Optimal Multiuser Detection: Interleave-Division Multiple-Access

Li Ping, Lihai Liu, and W. K. Leung
Department of Electronic Engineering
City University of Hong Kong
Hong Kong
eeliping@cityu.edu.hk

***Abstract*—This paper presents an asynchronous interleave-division multiple-access (IDMA) scheme, in which users are distinguished by different chip-level interleaving methods instead of by different signatures as in a conventional code-division multiple-access (CDMA) scheme. A very low-cost iterative detection algorithm is derived for the IDMA scheme based on a chip-by-chip detection principle. The proposed scheme can achieve nearly optimal performance for systems with a large number of users. Furthermore, receiver simplicity as well as high performance can be maintained in multipath environments.**

Keywords-CDMA; ISI channels; Iterative decoding; multiuser detection.

I. INTRODUCTION

Recently, significant progress has been made on turbo-type multiuser detection (MUD) for code-division multiple-access (CDMA) systems [1]-[6]. However, performance and complexity are still of major concerns. Moreover, a considerable gap continues to exist between the achieved performance [1]-[6] and the theoretical limits [7] of multiple access channels.

The use of signature sequences for user separation is a characteristic feature for a conventional CDMA system. Interleaving, which is usually placed between forward error correction (FEC) coding and spreading, is employed to combat fading effect. The possibility of employing interleaving for user separation in CDMA systems is briefly mentioned in [1]. In [8] and [9], the performance improvement by assigning different interleavers to different users in a CDMA system is demonstrated. In [10], multiuser detection in narrowband applications with a small number of users is investigated. A bandwidth-efficient trellis coded-modulation (TCM) system is made user-specific by selecting a unique combination of trellis code structure, interleaver and modulation constellation.

This paper presents a novel approach to asynchronous spread-spectrum mobile systems which we call interleave-division multiple-access (IDMA) [11]. In an IDMA scheme, users are distinguished by different chip-level interleaving methods instead of by different signatures as in a conventional CDMA system. Being a wideband scheme, IDMA inherits many advantages from CDMA, in particular, diversity against fading and mitigation of other-cell user interference.

A special benefit of IDMA is that it allows a very simple (and near-optimal) chip-by-chip iterative multiuser detection strategy. The normalized cost (per user) of this algorithm is independent of the number of users. Furthermore, such low complexity and high performance attributes can be maintained in a multipath environment.

The advantage of combining FEC and spreading using low-rate codes has been considered [12]. Such low-rate codes may lead to an improved coding gain and so improved cellular performance. We will demonstrate that the performance of the IDMA scheme based on low-rate turbo-Hadamard codes [13] is close to the corresponding Shannon limit [7].

The chip-by-chip detection algorithm described in this paper may also be applied to a conventional CDMA system, but in this case its performance is hampered by a correlation problem. We will explain this problem using a factor graph approach in the Appendix.

II. TRANSMITTER AND RECEIVER PRINCIPLES

A. Transmitter Structure

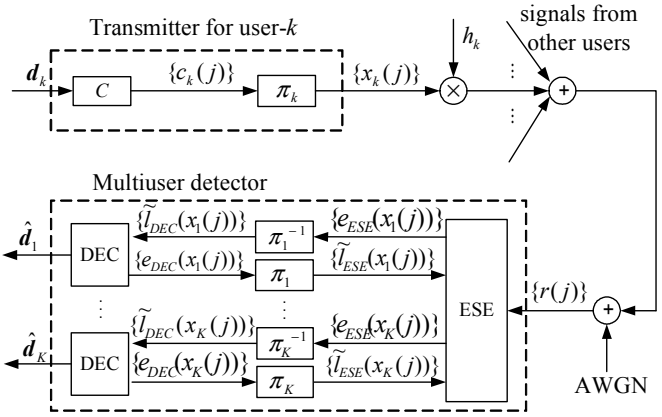

Fig. 1. Transmitter and receiver structures of the IDMA scheme, where π_k is the interleaver of user-k and K is the number of simultaneous users.

The upper part of Fig. 1 shows the transmitter structure of the proposed IDMA scheme with K simultaneous users. The input data sequence $\boldsymbol{d}_k$ of user-k is encoded by a low-rate code C (a spreading operation can be incorporated) into $\boldsymbol{c}_k = \{c_k(j), j = 1, \ldots, J\}$, where J is the frame length. A chip level interleaver π_k is then used, producing $\boldsymbol{x}_k = \{x_k(j), j = 1, \ldots, J\}$. (Note: We follow the convention of CDMA and call the elements in $\boldsymbol{c}_k$ and $\boldsymbol{x}_k$ "chips".) The key principle of the scheme is that the interleavers $\{\pi_k\}$ should be different for different users. We

assume that the interleavers are generated independently and randomly.

Assuming quasi-static single-path channels, after sampling at the chip rate, the received signal from K users can be written as

$$r(j) = \sum_{k=1}^{K} h_k x_k(j) + n(j), \qquad j = 1, 2, \ldots, J, \qquad (1)$$

where $x_k(j)$ is the jth chip transmitted by user-k, h_k the channel coefficient for user-k and $\{n(j)\}$ are samples of a zero-mean additive white Gaussian noise (AWGN) with variance $\sigma^2 = N_0/2$. We assume that the channel coefficients $\{h_k\}$ are known *a priori* at the receiver side.

B. Receiver Structure

The receiver operation is based on two constraints: the multiple access channel constraint and the code constraint of C. Finding an optimal solution is usually prohibitively complicated. An alternative suboptimal receiver structure is illustrated in the lower part of Fig. 1. It employs a low-cost chip-by-chip detection strategy which avoids conventional MAP [1][2] or matrix operations [3]. The receiver consists of an elementary signal estimator (ESE) and K *a posteriori* probability (APP) decoders (DECs), one for each user. The two constraints are considered separately in the ESE and in the DECs, and the results are then combined using a turbo-type iterative process [14]. This greatly reduces the complexity involved. The DECs produce hard decisions $\{\hat{\boldsymbol{d}}_k, \forall k\}$ on information bits $\{\boldsymbol{d}_k, \forall k\}$ during the final iteration.

Denote the *a priori* logarithm likelihood ratios (LLRs) about $\{x_k(j), \forall k, j\}$ by

$$\tilde{l}(x_k(j)) \equiv \log\left(\frac{\Pr(x_k(j)=+1)}{\Pr(x_k(j)=-1)}\right), \quad \forall\, k, j. \qquad (2)$$

These *a priori* LLRs are further distinguished by subscripts, i.e., $\tilde{l}_{ESE}(x_k(j))$ and $\tilde{l}_{DEC}(x_k(j))$, depending on whether they are used in the ESE or DECs.

The ESE uses $\{r(j)\}$ and $\{\tilde{l}_{ESE}(x_k(j))\}$ as its inputs and only the multiple access channel constraint is considered here. Given $\boldsymbol{h} = \{h_k, \forall k\}$, the corresponding *a posteriori* LLRs about $\{x_k(j), \forall k, j\}$ are defined by

$$\log\left(\frac{\Pr(x_k(j)=+1 \mid r(j), \boldsymbol{h})}{\Pr(x_k(j)=-1 \mid r(j), \boldsymbol{h})}\right) = \underbrace{\log\left(\frac{p(r(j) \mid x_k(j)=+1, \boldsymbol{h})}{p(r(j) \mid x_k(j)=-1, \boldsymbol{h})}\right)}_{e_{ESE}(x_k(j))} + \tilde{l}_{ESE}(x_k(j)) \qquad (3)$$

where $e_{ESE}(x_k(j))$ is the extrinsic LLR about $x_k(j)$ based on the channel observation and the *a priori* information of the other chips (excluding $x_k(j)$), as detailed in II.C.

Similarly, given $(\tilde{\boldsymbol{L}}_{DEC})_k \equiv \{\tilde{l}_{DEC}(x_k(j)), \forall j\}$ as the inputs to the DEC for user-k, the *a posteriori* LLRs about $\{x_k(j), \forall k, j\}$ are generated based on the code constraint of C as

$$\log\left(\frac{\Pr(x_k(j)=+1 \mid C, (\tilde{\boldsymbol{L}}_{DEC})_k)}{\Pr(x_k(j)=-1 \mid C, (\tilde{\boldsymbol{L}}_{DEC})_k)}\right)$$

$$= \underbrace{\log\left(\frac{\Pr(x_k(j)=+1 \mid C, (\tilde{\boldsymbol{L}}_{DEC})_k \setminus \tilde{l}_{DEC}(x_k(j)))}{\Pr(x_k(j)=-1 \mid C, (\tilde{\boldsymbol{L}}_{DEC})_k \setminus \tilde{l}_{DEC}(x_k(j)))}\right)}_{e_{DEC}(x_k(j))} + \tilde{l}_{DEC}(x_k(j)). \qquad (4)$$

where $(\tilde{\boldsymbol{L}}_{DEC})_k \setminus \tilde{l}_{DEC}(x_k(j))$ is obtained by setting $\tilde{l}_{DEC}(x_k(j)) = 0$ in $(\tilde{\boldsymbol{L}}_{DEC})_k$. The outputs of the DEC for the user-k consist of the extrinsic LLRs $\{e_{DEC}(x_k(j))\}$ shown in (4).

During the turbo-type iterative process, the extrinsic information generated by the ESE/DEC is used (after appropriate deinterleaving/interleaving) as the *a priori* information in the DEC/ESE, i.e., the updates $\{e_{ESE}(x_k(j))\} \Rightarrow \{\tilde{l}_{DEC}(x_k(j))\}$ and $\{e_{DEC}(x_k(j))\} \Rightarrow \{\tilde{l}_{ESE}(x_k(j))\}$ are performed at the ESE/DEC interface, see Fig. 1. Suppose that we start from the ESE. All $\{\tilde{l}_{ESE}(x_k(j))\}$ are initialized to zero, assuming that there is no initial *a priori* information.

The APP decoding in the DEC is a standard function [13][14], so we will not discuss it in detail. In the following, we will focus on the ESE.

C. Detailed Descriptions of the ESE

The ESE generates coarse estimates of $\{x_k(j), j = 1, \ldots, J, k = 1, \ldots, K\}$. We ignore the constraint of C in the ESE to maintain low complexity. Consider the jth chip of user-k with $x_k(j) \in \{+1, -1\}$ under BPSK modulation. We treat $x_k(j)$ as a random variable and use $e_{DEC}(x_k(j))$ to approximately update the *a priori* LLR $\tilde{l}_{ESE}(x_k(j))$ about $x_k(j)$. Then from (2), we have [3]

$$\mathrm{E}(x_k(j)) = \frac{\exp(\tilde{l}_{ESE}(x_k(j))) - 1}{\exp(\tilde{l}_{ESE}(x_k(j))) + 1} = \tanh(\tilde{l}_{ESE}(x_k(j))/2) \qquad (5)$$

$$\mathrm{Var}(x_k(j)) = 1 - (\mathrm{E}(x_k(j)))^2 \qquad (6)$$

where $\mathrm{E}(x)$ and $\mathrm{Var}(x)$ denote the mean and variance of x, respectively.

For user-k, denoting $\zeta_k(j) = \sum_{\substack{k'=1 \\ k' \neq k}}^{K} h_{k'} x_{k'}(j) + n(j)$, we can rewrite (1) as

$$r(j) = h_k x_k(j) + \zeta_k(j). \qquad (7)$$

The Gaussian Approximation: Assume that $\{x_k(j), \forall k\}$ are independent and identically distributed (i.i.d.) random variables. Applying the central limit theorem, $\zeta_k(j)$ in (7) can be approximated by a Gaussian random variable with mean and variance

$$\mathrm{E}(\zeta_k(j)) = \sum_{\substack{k'=1 \\ k' \neq k}}^{K} h_{k'} \mathrm{E}(x_{k'}(j)) \qquad (8a)$$

$$\mathrm{Var}(\zeta_k(j)) = \sum_{\substack{k'=1 \\ k' \neq k}}^{K} |h_{k'}|^2 \mathrm{Var}(x_{k'}(j)) + \sigma^2. \qquad (8b)$$

Applying the Gaussian approximation to (7), $e_{ESE}(x_k(j))$ in (3) can be calculated as

$$\begin{aligned} e_{ESE}(x_k(j)) &= \log \frac{\exp\left(-\frac{(r(j)-\mathrm{E}(\zeta_k(j))-h_k)^2}{2\mathrm{Var}(\zeta_k(j))}\right)}{\sqrt{2\pi\mathrm{Var}(\zeta_k(j))}} \\ &\quad - \log \frac{\exp\left(-\frac{(r(j)-\mathrm{E}(\zeta_k(j))+h_k)^2}{2\mathrm{Var}(\zeta_k(j))}\right)}{\sqrt{2\pi\mathrm{Var}(\zeta_k(j))}} \\ &= 2h_k \cdot \frac{r(j)-\mathrm{E}(\zeta_k(j))}{\mathrm{Var}(\zeta_k(j))} \\ &= 2h_k \cdot \frac{r(j)-\mathrm{E}(r(j))+h_k\mathrm{E}(x(j))}{\mathrm{Var}(r(j))-|h_k|^2\mathrm{Var}(x(j))} \end{aligned} \quad (9)$$

where (based on (1))

$$\mathrm{E}(r(j)) = \sum_{k'=1}^{K} h_{k'}\mathrm{E}(x_{k'}(j)) \quad (10a)$$

$$\mathrm{Var}(r(j)) = \sum_{k'=1}^{K} |h_{k'}|^2 \mathrm{Var}(x_{k'}(j)) + \sigma^2 . \quad (10b)$$

D. A Summary of the Chip-by-Chip Detection Algorithm

For clarity, we summarize the chip-by-chip detection algorithm as follows (with $\{\tilde{l}_{ESE}(x_k(j)),\ \forall k, j\}$ initialized to zero).

ESE operations:

$$\mathrm{E}(x_k(j))) \Leftarrow \tanh(\tilde{l}_{ESE}(x_k(j))/2), \qquad \forall k, j. \ (11a)$$

$$\mathrm{Var}(x_k(j)) \Leftarrow 1-(\mathrm{E}(x_k(j)))^2, \qquad \forall k, j. \ (11b)$$

$$\mathrm{E}(r(j)) \Leftarrow \sum_{k'=1}^{K} h_{k'}\mathrm{E}(x_{k'}(j)), \qquad \forall j. \ (12a)$$

$$\mathrm{Var}(r(j)) \Leftarrow \sum_{k'=1}^{K} |h_{k'}|^2 \mathrm{Var}(x_{k'}(j)) + \sigma^2, \qquad \forall j. \ (12b)$$

$$e_{ESE}(x_k(j)) \Leftarrow 2h_k \cdot \frac{r(j)-\mathrm{E}(r(j))+h_k\mathrm{E}(x_k(j))}{\mathrm{Var}(r(j))-|h_k|^2\mathrm{Var}(x_k(j))}, \ \forall k, j. \ (13)$$

DEC operations:

The APP decoding in the DECs is performed to generate $\{e_{DEC}(x_k(j))\}$. Update $\{e_{DEC}(x_k(j))\} \Rightarrow \{\tilde{l}_{ESE}(x_k(j))\}$, then go back to (11) for the next iteration.

The detection/decoding algorithm can be carried out either by a parallel schedule (listed above), in which the operations (11)-(13) and the APP decoding are carried out simultaneously for all users, or by a serial schedule, in which the operations (11)-(13) and after the APP decoding are carried out user by user. With the serial detection algorithm, the means and variances in (12) are partially updated after the APP decoding for user-*k* is completed.

The normalized computational cost in (11)–(13) (excluding the APP decoding of *C*) is only about 6 additions, 6 multiplications and a tanh(*x*) function per chip per user per iteration. This complexity is very low and is independent of user number *K*.

III. Chip-by-Chip Estimation in Multipath Channels

We now consider MUD in more complicated asynchronous multipath channels. The overall decoder structure is the same as that shown in Fig. 1 and so the iterative principle discussed in Section II is still applicable. Therefore, we will only focus on the calculation of $e_{ESE}(x_k(j))$.

A. Discrete Signal Model in Multipath Fading Channels

Consider a multiple access system with *K* simultaneous users over quasi-static multipath fading channels with *L* tap-coefficients. Let $\{h_{k,0}, \cdots, h_{k,L-1}\}$ be the fading coefficients related to user-*k*. After sampling at the chip rate, the signal at the receiver can be represented by

$$r(j) = \sum_{k=1}^{K}\sum_{l=0}^{L-1} h_{k,l}x_k(j-l) + n(j), \qquad \forall j. \quad (14)$$

For simplicity, we still assume real signaling. The principle can be generalized to complex signaling.

B. The Rake Gaussian (RG) Approach

For a multipath channel with *L* tap-coefficients, a transmitted chip $x_k(j)$ is observed on *L* successive samples $\{r(j), r(j+1), \ldots, r(j+L-1)\}$ in the received signal. A rake-type operation can be applied to combine the information about $x_k(j)$ from these samples. We summarize the rake Gaussian (RG) algorithm below. Only ESE operations are listed since DEC operations are exactly the same as those listed in II.

$$\mathrm{E}(x_k(j)) \Leftarrow \tanh(\tilde{l}_{ESE}(x_k(j))/2), \qquad \forall k, j. \ (15a)$$

$$\mathrm{Var}(x_k(j)) \Leftarrow 1-(\mathrm{E}(x_k(j)))^2, \qquad \forall k, j. \ (15b)$$

$$\mathrm{E}(r(j)) \Leftarrow \sum_{k=1}^{K}\sum_{l=0}^{L-1} h_{k,l}\mathrm{E}(x_k(j-l)), \qquad \forall j. \ (16a)$$

$$\mathrm{Var}(r(j)) \Leftarrow \sum_{k=1}^{K}\sum_{l=0}^{L-1} |h_{k,l}|^2 \mathrm{Var}(x_k(j-l)) + \sigma^2, \quad \forall j. \ (16b)$$

$$e_{ESE}(x_k(j))_l \Leftarrow 2h_{k,l} \cdot \frac{r(j+l)-\mathrm{E}(r(j+l))+h_{k,l}\mathrm{E}(x_k(j))}{\mathrm{Var}(r(j+l))-|h_{k,l}|^2\mathrm{Var}(x_k(j))}, \ \forall k, j, l. \ (17)$$

$$e_{ESE}(x_k(j)) \approx \sum_{l=0}^{L-1} e_{ESE}(x_k(j))_l, \qquad \forall k, j. \ (18)$$

Some explanations about (15) – (18) are in order.

- $\mathrm{E}(r(j))$ and $\mathrm{Var}(r(j))$ in (16) involve the signals subject to multiple delays.
- $e_{ESE}(x_k(j))_l$ in (17) is the partial extrinsic LLR about $x_k(j)$ calculated from $r(j+l)$.

- Equation (18) assumes that the partial extrinsic LLR $\{(e_{ESE}(x_k(j)))_l\}$ are based on independent observations. However, the related observations $\{r(j+l), l = 0, 1, \ldots, L\text{-}1\}$ are actually correlated and so (18) is only an approximation.
- The complexity of the RG algorithm for a L-tap multipath channel is about L times that for a single-path channel.

C. Generalization

- The transmitted signals can be complex (e.g., QPSK modulation). The channel coefficients $\{h_{k,l}\}$ can also be complex. The operations (15)–(18) should be modified slightly for every chip in the real or imaginary part, but the main principle remains the same.
- The channel coefficients $\{h_{k,l}\}$ can also be time-varying. In this case, we only need to replace $\{h_{k,l}\}$ in (15)–(18) with time-indexed coefficients (such as $\{h_{k,l}(j)\}$).
- When multiple receive antennas are used, there are more observations with respect to each $x_k(j)$. The rake receiver function can be extended to combine the estimates from all receive antennas. The principle is very similar to that for multipath channels.

IV. Numerical Results

In this section, simulation results are provided to illustrate the performance of IDMA systems based on the MUD algorithms derived above.

We first examine the throughput efficiency of the proposed IDMA scheme based on an experimental system. A rate-1/2 convolutional code with generator polynomials $(23, 35)_8$ is used for all users. The block size of each user is 128 information bits. The coded length is 256+8, where eight extra bits are used for termination. The coded bits are spread by a length-8 spreading sequence [+1, −1, +1, −1, +1, −1, +1, −1] and interleaved by two independent interleavers to produce two chip streams for the in-phase and quadrature parts. All of the interleavers are generated randomly and independently. The serial algorithms are assumed. The rate (including spreading but ignoring tailing bits) for each user is $R_C = 1/16$ information bits per symbol. The total system throughput is $K \times R_C$ that is a measurement of the overall bandwidth efficiency.

Fig. 2 shows the performance of the above IDMA system in AWGN channels with different numbers of simultaneous users using the chip-by-chip detection algorithm in II. One receiver antenna is used. Five iterations are used for the results with $K \le 24$, and 10 iterations for $K = 32$. Near single-user performance is achievable for very large K. Notice that $K = 32$ is four times the length of the spreading sequence. The corresponding system throughput is $K \times R_C = 2$ information bits per chip. Fig. 3 shows the performance using the RG algorithm in quasi-static frequency-nonselective Rayleigh fading multipath channels with different numbers of tap-coefficients. These coefficients remain constant within a frame of 2112 (= (128×2+8)×8) chips. The number of simultaneous users is K = 32. The system throughput = 2 information bits per chip. From Fig. 3, performance improves uniformly with increasing path number due to the improved diversity. Fig. 4 shows the performance with one and two receive antennas in multipath channels with two tap-coefficients. It is rather surprising to see that the system throughput can be as high as 6 information bits per chip with two receive antennas (when K = 96) with performance still close to the single-user oe at BER = 10^{-4}.

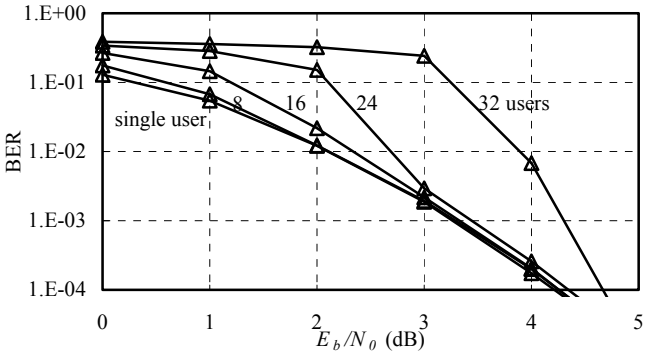

Fig. 2. Performance of a convolutionally coded IDMA system in AWGN channels.

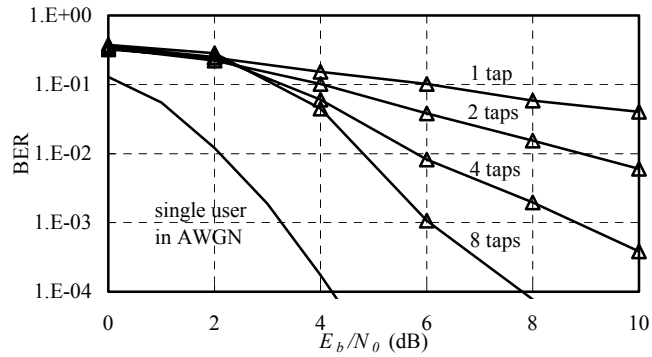

Fig. 3. Performance of a convolutionally coded IDMA system in quasi-static frequency-nonselective Rayleigh fading multipath channels. Iteration number = 5, K = 32.

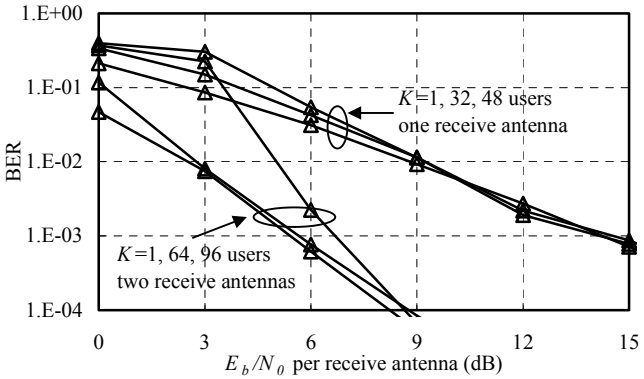

Fig. 4. Performance of a convolutionally coded IDMA system in quasi-static frequency-nonselective Rayleigh fading multipath channels with single and two receive antennas. Iteration number = 8, L = 2.

Next we consider the power efficiency of the proposed scheme. In this case, good low-rate codes should be employed to maximize the coding gain. We adopt a rate-0.0581 turbo-Hadamard code [13] with an information length of 4095 bits per user. (It is constructed by concatenating 3 convolutional-Hadamard codes, each of which is generated from a length-32 Hadamard code and a convolutional code with polynomial $G(x) = 1/(1+x)$. The information bits in all component codes except one are punctured.) Fig. 5 shows the simulated performance. BPSK signaling and an AWGN channel model are assumed. From Fig. 5, performance of BER = 10^{-5} is observed at $E_b/N_0 \approx 1.1$ dB with $K = 8$. This corresponds to a total system rate of $K \times R_C = 0.465$. This is only about 1.22 dB away from the corresponding Shannon limit, which is $E_b/N_0 = -0.12$ dB for $K \times R_C = 0.465$, the same as that for a single-user real AWGN channel [7].

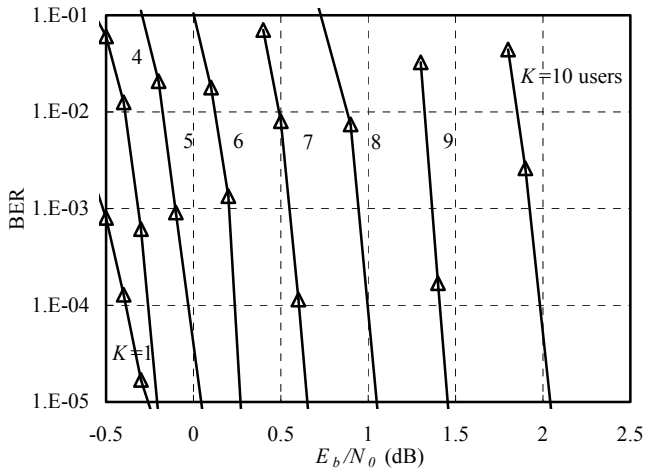

Fig. 5. Performance of an IDMA system based on interleaved turbo-Hadamard codes [13] over AWGN channels. User number K is marked in the figure. Iteration number = 30.

V. Conclusions

We have introduced an IDMA scheme that allows very low-cost multiuser detection. The basic principle is to use interleavers for user separation. A very large number of users can be processed with modest computing power. Multipath is no longer a serious issue as far as complexity is concerned. Near-capacity performance is observed for multiple access channels.

Appendix : A Factor Graph Approach

In [15], an elegant multiuser detection scheme is described using Tanner graphs. The principle in [15] can be generalized and applied to both CDMA and IDMA schemes. We give factor-graph [16] representations of CDMA and IDMA at chip level to provide insight into their similarities and differences.

The factor graphs for CDMA and IDMA schemes given in Fig. 6 consist of variable nodes (black nodes) for transmitted chips $\{x_k(j)\}$, observation nodes (dashed ovals) for observations $\{r(j)\}$ and constraint nodes (squares) for the relationship that all chips connecting to a common constraint node belong to the same frame of a spreading sequence. For clarity, some extremely simplified parameters are used here:

- User number $K = 2$ and no ISI (see (1)).
- No FEC code (so each variable node is connected to only one constraint node representing a spreading relationship).

The principle can easily be generalized to systems with more users.

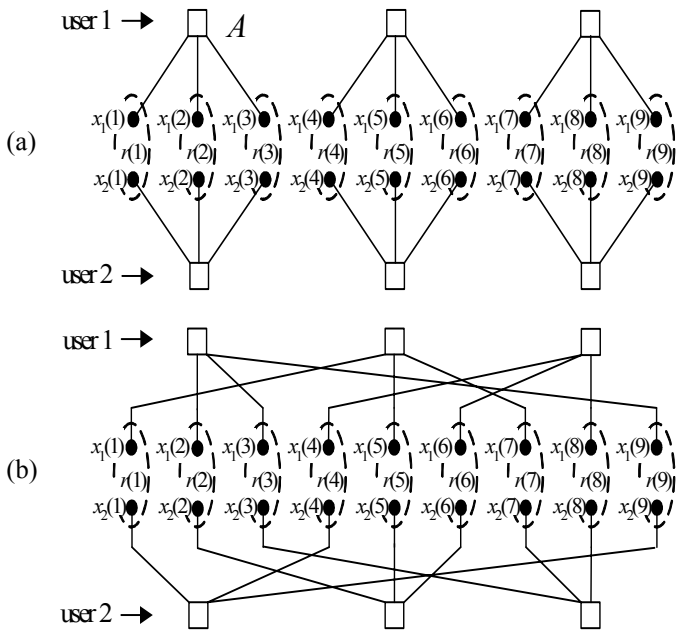

Fig. 6. (a) A factor graph for a conventional CDMA scheme and (b) a factor graph for an IDMA scheme, where the black nodes inside an oval are related by $r(j) = h_1 x_1(j) + h_2 x_2(j) + n(j)$, i.e., equation (1) with $K = 2$. Notice that (a) and (b) are different only in the connection of their edges.

A message passing process for factor graphs [16] can be applied in the proposed chip-by-chip detection. Two types of messages are defined:

- A message from a variable node to a constraint node is defined as $e_{ESE}(x_k(j))$.
- A message from a constraint node to a variable node is defined as $e_{DEC}(x_k(j))$.

The operations on variable nodes involve the ESE operations (e.g., those defined in (11)-(13) for generating $\{e_{ESE}(x_k(j))\}$ and those on constraint nodes involve the APP decoding for generating $\{e_{DEC}(x_k(j))\}$.

The main difference between the factor graph in Fig. 6 and the Tanner graph used in [15] is at the constraint nodes. In [15], each constraint node represents a single-parity-check relationship. For the factor graph in Fig. 6, each constraint node represents a spreading operation. For example, let $\boldsymbol{s}=[s_1,$

s_2, s_3] be the spreading sequence for user-1 in Fig. 6(a). Let the spreading operation be $c_1 \rightarrow c_1 \cdot \boldsymbol{s}$ where c_1 is the first bit to be spread. The values of the variable nodes connected to constraint node A in Fig. 6(a) are given as: $x_1(1) = c_1 \cdot s_1$, $x_1(2) = c_1 \cdot s_2$ and $x_1(3) = c_1 \cdot s_3$. Therefore the constraint represented by A is

$$x_1(1)/s_1 = x_1(2)/s_2 = x_1(3)/s_3 .$$

This represents a much stronger constraint than the single-parity-check relationship. It makes the systems in Fig. 6 more robust against interference, so that a large number of users can be supported.

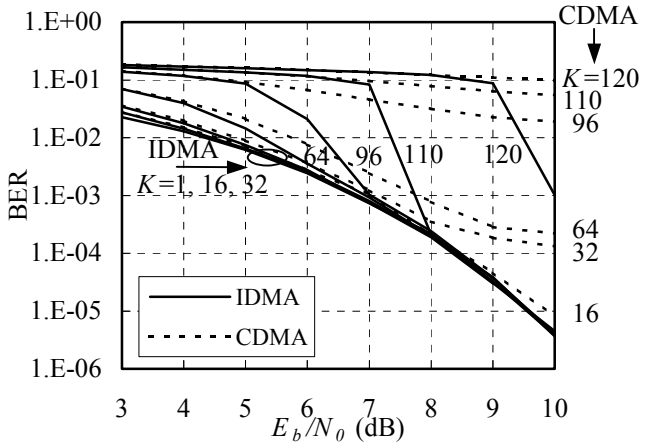

Fig. 7. Performance of un-coded CDMA and IDMA systems over AWGN channels. Spreading length = 64. The user number K is marked in the figure. The iteration number is 10 for both CDMA and IDMA.

The difference between CDMA and IDMA lies at the edge connections. In a conventional synchronous CDMA, frames of different users overlap each other. This results in short cycles in the factor graph (see Fig. 6(a)), which has a detrimental effect on a message passing process [17]. For IDMA, the randomized edge connection greatly reduces the number of short cycles (see Fig. 6(b)). This is essential for the success of a message passing process.

As an illustration, Fig. 7 shows the performance of un-coded CDMA and IDMA systems in AWGN channels with the serial chip-by-chip detection algorithm. The spreading ratio is 64 for both CDMA (with randomly generated length-64 signature sequences) and IDMA (with randomly generated interleavers and a length-64 spreading sequence [+1, –1, +1, –1, …] for all users). The length of the information block is 256 bits per user. It is observed that near single-user performance is achieved in the IDMA system even for K = 110 (measured at BER = 10^{-4}) while it does not perform well in the conventional CDMA system.

As a final note, the results presented in Fig. 7 are based on real signaling. The user number can be doubled if complex signaling is used.

ACKNOWLEDGMENT

This work was fully supported by a grant from the Research Grant Council of the Hong Kong SAR, China [Project No. CityU 1110/00E].

REFERNCES

[1] M. Moher, "An iterative multiuser decoder for near-capacity communications," *IEEE Trans. Commun.*, vol. 46, pp. 870–880, July 1998.

[2] M. C. Reed, C. B. Schlegel, P. D. Alexander, and J. A. Asenstorfer, "Iterative multiuser detection for CDMA with FEC: Near-single-user performance," *IEEE Trans. Commun.*, vol. 46, pp. 1693–1699, Dec. 1998.

[3] X. Wang and H. V. Poor, "Iterative (turbo) soft interference cancellation and decoding for coded CDMA," *IEEE Trans. Commun.*, vol. 47, pp. 1046–1061, July 1999.

[4] A. AlRustamani, A. D. Damnjanovic, and B. R. Vojcic, "Turbo greedy multiuser detection," *IEEE J. Select. Areas Commun*, vol. 19, pp. 1638–1645, Aug. 2001.

[5] J. Boutros and G. Carie, "Iterative multiuser joint decoding: Unified framework and asymptotic analysis," *IEEE Trans. Inform.Theory*, vol. 48, pp. 1772–1793, July 2002.

[6] Z. Shi and C. Schlegel, "Joint iterative decoding of serially concatenated error control coded CDMA," *IEEE J. Select. Areas Commun.* vol. 19, pp. 1646–1653, Aug. 2001.

[7] S. Verdú, "The capacity region of the symbol-asynchronous Gaussian multiple-access channel," *IEEE Trans. Inform. Theory*, vol. 35, pp. 733–751, July 1989.

[8] S. Brück, U. Sorger, S. Gligorevic, and N. Stolte, "Interleaving for outer convolutional codes in DS-CDMA Systems," *IEEE Trans. Commun.*, vol. 48, pp. 1100–1107, July 2000.

[9] A. Tarable, G. Montorsi, and S. Benedetto, "Analysis and design of interleavers for CDMA systems," *IEEE Commun. Lett.*, vol. 5, pp. 420–422, Oct. 2001.

[10] F. N. Brannstrom, T. M. Aulin, and L. K. Rasmussen, "Iterative multi-user detection of trellis code multiple access using a posteriori probabilities," in *Proc. ICC 2001*, Finland, June 2001, pp. 11–15.

[11] Li Ping, K. Y. Wu, and L. Liu, "A simple, unified approach to nearly optimal multiuser detection and space-time coding," in *ITW 2002*, India, Oct. 2002, available: http://www.ee.cityu.edu.hk /~liping.

[12] P. Frenger, P. Orten, and T. Ottosson, **"**Code-spread CDMA using maximum free distance low-rate convolutional codes," *IEEE Trans. Commun.*, vol. 48, pp. 135–144, Jan. 2000.

[13] Li Ping, W. K. Leung, and K. Y. Wu, "Low-rate turbo-Hadamard codes," submitted for publication, available: http://www.ee.cityu.edu.hk /~liping/research.

[14] C. Berrou and A. Glavieux, "Near Shannon limit error correcting coding and decoding: Turbo-codes," *IEEE Trans. Commun.*, vol. 44, pp. 1261–1271, Oct. 1996.

[15] R. J. McEliece, "Are turbo-like codes effective on nonstandard channels?" *IEEE Inform. Theory Society Newsletter*, vol. 51, no.4, pp. 1–8, Dec. 2001.

[16] F. E. Kschischang, B. J. Frey, and H.-A. Loeliger, "Factor graphs and the sum-product algorithm," *IEEE Trans. Inform. Theory*, vol. 47, pp. 498–519, Feb. 2001.

[17] Y. Mao and A. H. Banihashemi, "A heuristic search for good low-density parity-check codes at short block lengths," in *Proc. ICC 2001*, Finland, June 2001, pp. 41–44.